Simultaneous determination of mean pressure and deviatoric stress based on numerical tensor analysis: a case study for polycrystalline x-ray diffraction of gold enclosed in a methanol–ethanol mixture

2006 J. Phys.: Condens. Matter 18 S979

(http://iopscience.iop.org/0953-8984/18/25/S06)

INSTITUTE OF PHYSICS PUBLISHING JOURNAL OF PHYSICS: CONDENSED MATTER

J. Phys.: Condens. Matter **18** (2006) S979–S994 doi:10.1088/0953-8984/18/25/S06

Simultaneous determination of mean pressure and deviatoric stress based on numerical tensor analysis: a case study for polycrystalline x-ray diffraction of gold enclosed in a methanol–ethanol mixture

A Yoneda[1,3] **and A Kubo**[2]

[1] Institute for Study of the Earth's Interior, Okayama University, Misasa, Tottori 682-0193, Japan
[2] Department of Geosciences, Princeton University, Princeton, NJ 08544, USA

E-mail: yoneda@misasa.okayama-u.ac.jp

Received 1 December 2005, in final form 26 April 2006
Published 8 June 2006
Online at stacks.iop.org/JPhysCM/18/S979

Abstract

It is known that the {100} and {111} planes of cubic crystals subjected to uniaxial deviatoric stress conditions have strain responses that are free from the effect of lattice preferred orientation. By utilizing this special character, one can unambiguously and simultaneously determine the mean pressure and deviatoric stress from polycrystalline diffraction data of the cubic sample. Here we introduce a numerical tensor calculation method based on the generalized Hooke's law to simultaneously determine the hydrostatic component of the stress (mean pressure) and deviatoric stress in the sample. The feasibility of this method has been tested by examining the experimental data of the Au pressure marker enclosed in a diamond anvil cell using a pressure medium of methanol–ethanol mixture. The results demonstrated that the magnitude of the deviatoric stress is ∼0.07 GPa at the mean pressure of 10.5 GPa, which is consistent with previous results of Au strength under high pressure. Our results also showed that even a small deviatoric stress (∼0.07 GPa) could yield a ∼0.3 GPa mean pressure error at ∼10 GPa.

1. Introduction

Deviatoric stress could cause inhomogeneous strain responses on each *hkl* plane in materials [1, 2]. This effect could cause a systematic error in the pressure value if the pressure is determined from the unit cell volume of pressure standard materials using x-ray diffraction [3, 4]. On the other hand, by utilizing this effect, polycrystalline materials of cubic symmetry have extensively been investigated to estimate the stress state of the sample

[3] Author to whom any correspondence should be addressed.

compressed by opposed anvil high-pressure cells through radial diffraction [1, 4–21] and axial diffraction [3, 22–25] geometries.

Many of the above studies have employed analytical methods based on the following theoretical relationships established in the x-ray elastic constant (XEC) method [26, 27] to analyse the magnitude of deviatoric stress in the sample,

$$d_m(hkl) = d_p(hkl)\{1 + (1 - 3\cos^2\psi)Q(hkl)\}, \tag{1}$$

where $d_m(hkl)$ and $d_p(hkl)$ are the d-spacing observed in x-ray measurements and that caused by mean pressure alone, respectively, ψ is the angle between the load axis of the deviatoric stress and the diffracting plane normal, and Q is a factor containing the magnitude of the deviatoric stress and the single crystal elastic compliances, S_{ij}. Note that equation (1) is derived under the assumption of isotropic grain orientation. If the sample had preferred orientation, the deviatoric stress analysed from equation (1) could have additional uncertainty that cannot be analytically estimated. However, it is known that the hkl planes of four-fold and three-fold symmetries, such as {100} and {111}, respectively, have strain responses that are free from the effect of lattice preferred orientation [28, 29]. Therefore, by using only these reflections for data analysis, one can unambiguously determine the deviatoric stress in a sample placed in a uniaxial stress field.

On the other hand, as long as the single-crystal elastic constants of the sample are known and the deformation is in the elastic regime, we can directly determine the deviatoric stress of the sample from the strain observed in diffraction lines based on the generalized Hooke's law, as Weidner *et al* [30] suggested. In this work, we use the generalized Hooke's law instead of using equation (1) to examine the stress responses of cubic crystals in an axial symmetric stress field as a function of grain orientation by conducting numerical tensor calculations. The advantage of the numerical tensor calculation is that we can directly analyse the degree of variation of the stress response of the crystalline material as a function of grain orientation, which cannot be done from equation (1). Due to this reason, numerical tensor analysis could also be used to examine the lattice preferred orientation, although we will not attempt to do it in the present study.

In order to determine a 'real pressure' that is determined by taking all the hydrostatic stress components of the sample into account, Meng *et al* have suggested a simple analytical method. However, their method also assumes isotropic grain orientation. To eliminate any assumption related to preferred orientation of the sample, we introduce a numerical tensor analysis to simultaneously determine the mean pressure and deviatoric stress of a cubic sample compressed in a diamond anvil cell (DAC). The feasibility of this numerical method will be tested by examining the mean pressure and deviatoric stress of Au compressed in a DAC using a methanol–ethanol pressure transmitting medium. Au has been selected as the sample because it has been widely used as a pressure standard material (pressure marker) in high-pressure experimental physics and it has a large anisotropic factor, $a = 2.9$ at 0 GPa (here $a = 2C_{44}/(C_{11} - C_{12})$ with C_{ij} being the stiffness elastic constant).

2. Geometrical settings and notation of tensor

Figure 1 shows our experimental setting of angle-dispersive x-ray diffraction experiments using a DAC and an imaging plate (IP) detector with axial diffraction geometry. This geometry is assumed to develop our numerical calculation method. The X axis is in the direction of the normal vector of the diffracting planes. In this geometry, all crystallites for which an (hkl) plane is perpendicular to the X axis will contribute to the hkl diffraction peak. This family of crystallites includes crystallites with a variety of orientations (rotation around X). For simplicity, we set the Z' axis in the instrumental coordinate to be identical to the Z axis in

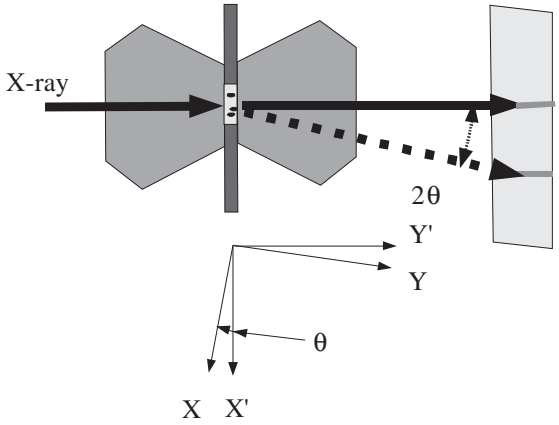

Figure 1. Schematic figure of the experimental configuration from a vertical viewpoint. The relationship between the instrumental coordinate system ($X'Y'Z'$) and the x-ray diffraction coordinate system (XYZ) is shown. Note that Z and Z' axes are perpendicular to the sheet. The x-ray beam proceeds along the Y' axis. Axial symmetry in the stress field is assumed with respect to the Y' axis. The X axis is set to be in the direction normal to each diffracting plane. The range of θ was 5°–10° in the present measurements. When the Y' axis is the load axis of the deviatoric stress, the angle ψ in equation (1) is given as $\psi = \pi/2 - \theta$.

the x-ray diffraction coordinate. Definitions of the angle θ and the relationship between the instrumental coordinates ($X'Y'Z'$) and the x-ray diffraction coordinates (XYZ) are also shown in figure 1. Figure 2 shows the definition of crystal rotation angle ϕ and the relative relationship between the crystal coordinates (xyz) and the x-ray diffraction coordinates (XYZ) for the representative cases of the {100} and {111} planes in a single crystal of cubic symmetry. The x-ray diffraction coordinates (XYZ) are dependent on each hkl plane in the angle-dispersive geometry, while if an energy-dispersive geometry with a fixed 2θ angle is employed, the x-ray diffraction coordinates (XYZ) in all of the hkl planes are the same for all the hkl planes.

We describe the stress and strain tensors using Voigt's notation using one Voigt index instead of the original tensor notation using pair of indices, ij. Thus, stress, σ, can be expressed as a six-component column vector:

$$\vec{\sigma} = \begin{pmatrix} \sigma_1 \\ \sigma_2 \\ \sigma_3 \\ \sigma_4 \\ \sigma_5 \\ \sigma_6 \end{pmatrix}. \tag{2}$$

The superscript arrow indicates that it is the six-component form of the second rank tensor. In this expression, based on Voigt's notation, σ_1, σ_2, and σ_3 are compressional stress components, and σ_4, σ_5, and σ_6 are shear stress ones. The mean pressure p is defined as the average of compressional stress components, $p = (\sigma_1 + \sigma_2 + \sigma_3)/3$. Mean pressure corresponds to the hydrostatic pressure component of the stress in the sample nonhydrostatically compressed in an opposed anvil cell that can be determined from radial x-ray diffraction experiments at the azimuthal angle $\psi = 54.7°$ [1, 2] under an assumption of isotropic crystal grain orientation. A hydrostatic pressure is a special state of stress, $\sigma_1 = \sigma_2 = \sigma_3$ and $\sigma_4 = \sigma_5 = \sigma_6 = 0$.

Considering the geometry of the experimental instruments, it is reasonable to assume a deviatoric stress $\vec{\Delta\sigma}$ with axial symmetry along the Y' axis:

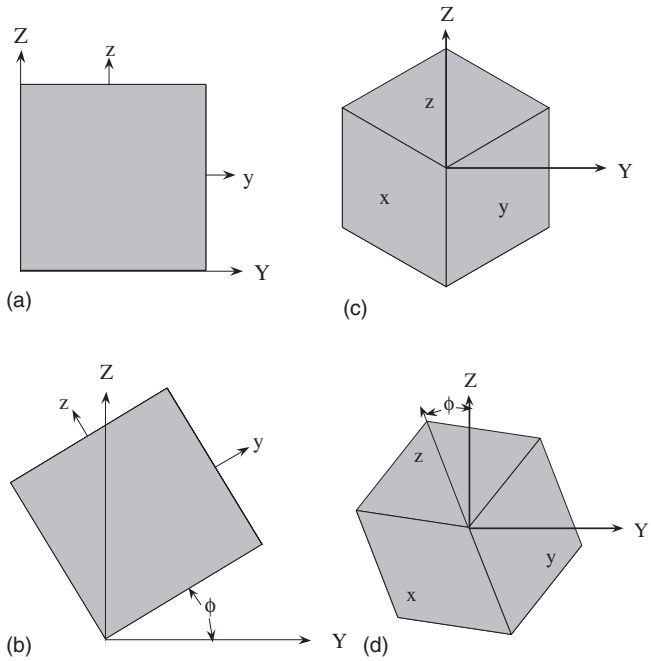

Figure 2. Schematic figure of the relation between the x-ray diffraction coordinate system (XYZ) and the crystal coordinate system (xyz). Note that the X axis is perpendicular to the sheet in every case, and ϕ is the anticlockwise rotation angle of the crystal along the X axis. (a) Typical setting for the {200} reflections. Note that the XYZ and xyz coordinates are identical in this case. (b) The crystal grain rotates by ϕ along the X axis from the typical setting for {200} reflections. This configuration also contributes to the {200} reflections. (c) Typical setting for the {111} reflections. Note that the xyz axes are normal to the faces labeled by the corresponding characters. (d) The crystal grain rotates by ϕ along the X axis from the typical setting for the {111} reflections. This configuration also contributes to the {111} reflections.

$$\vec{\Delta\sigma}_{X'X'Z'} = \begin{pmatrix} -\Delta\sigma/2 \\ \Delta\sigma \\ -\Delta\sigma/2 \\ 0 \\ 0 \\ 0 \end{pmatrix}, \tag{3}$$

where the subscript specifies the axial coordinates for the expression. The above expression is written in the instrumental ($X'Y'Z'$) coordinate system. When we express stresses in x-ray diffraction (XYZ) coordinates, they must be transformed according to the transformation rule for second rank tensors (see the appendix for details).

For convenience, we put forth the following definitions.

(1) The deviatoric stress tensor is defined such that it does not contain the mean pressure component, i.e.,

$$\sigma_1 + \sigma_2 + \sigma_3 \equiv 0, \tag{4}$$

which is an invariant with respect to the coordinate transformation. Note that equation (3) satisfies this requirement.

(2) The sign of the stress, and thus the strain, is defined to be positive for compression so that pressure is expressed as a positive number.

Also, from the viewpoint of elasticity, the strains in the hkl planes, (222), (200) and (220), for example, should be exactly the same as those of the (111), (100) and (110) planes, respectively. Since 100 and 110 diffraction lines of fcc Au are extinct, we use {200} and {220} to denote {100} and {110}, respectively, in the following text.

3. Elastic strain in cubic single crystal under deviatoric stress

Here we attempt to show the advantage of a numerical tensor calculation based on the generalized Hooke's law compared to the conventional XEC method using equation (1) to examine the elastic strain response of cubic materials under deviatoric stress. Also, we attempt to confirm the consistency of the results obtained by numerical tensor calculation with those obtained from equation (1).

For the purpose of schematic demonstration, we hypothetically apply a deviatoric stress normalized as $\Delta\sigma = 1$ GPa to Au at 0 GPa,

$$\vec{\Delta\sigma}_{X'X'Z'} = \begin{pmatrix} -1/2 \\ 1 \\ -1/2 \\ 0 \\ 0 \\ 0 \end{pmatrix}. \tag{5}$$

To calculate the strain response of all grains contributing to the diffraction peak as a function of grain orientation ϕ, we use the generalized Hooke's law,

$${}^{hkl}\varepsilon_X = {}^{hkl}\varepsilon_1 = \sum_{m=1}^{6} {}^{hkl}S_{XYZ}(\phi)_{1m}\vec{\Delta\sigma}_{XXZ}. \tag{6}$$

Here, ε_X is the ε_1 of $\vec{\varepsilon}$ expressed in the x-ray diffraction (XYZ) coordinate, because only the strain in the X direction, ε_X, is related to the x-ray diffraction measurement in the present x-ray diffraction geometry (figure 1). The ${}^{hkl}S_{XYZ}$ is derived from the usual compliance matrix expression S_{xyz} in the xyz crystal coordinate system through the coordinate transformation rule for a fourth-rank tensor (see the appendix for details including the derivation of $\vec{\Delta\sigma}_{XYZ}$).

Figure 3 shows the results of strain responses of four representative families of hkl planes as a function of grain orientation angle ϕ obtained from equation (6) based on the numerical tensor calculations. Strains for {111} and {200} are constant during the rotation around the X-axis, while those of {220} and {311} vary significantly. In other words, hkl planes of four-fold and three-fold symmetries, such as {100} and {111}, respectively, have strain responses that are free from the effect of lattice preferred orientation around the X axis. These results are consistent with the results by Gauthier [29]. This special property for {111} and {200} is the basis of our numerical analysis to simultaneously determine the mean pressure and deviatoric stress described later. Not only the deviation of the diffraction peak from the position expected in hydrostatic conditions, but also the broadening of peak width as implied in figure 3 would be recorded in the x-ray diffraction data. Both anomalies could be used to analyse the deviatoric stress in the x-ray diffraction data. However, in particular to use the latter information for deviatoric stress analysis, one might need to obtain diffraction data of very high angular resolution to distinguish the stress induced peak broadening from the instrumental one.

Figure 4 shows the results of numerical tensor calculation of the lattice strain response of Au as a function of grain orientation ψ. The calculation was carried out using a modified

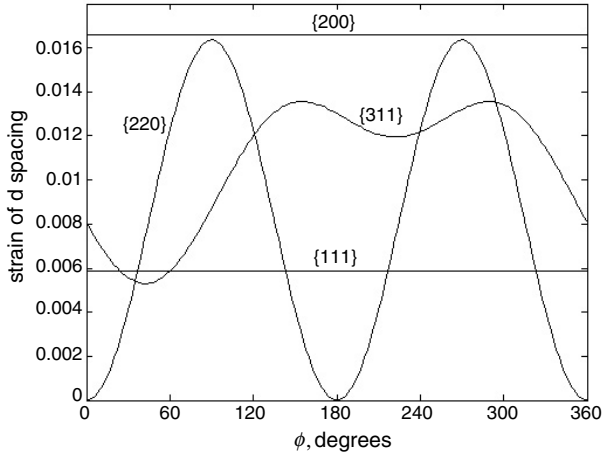

Figure 3. Variations in ${}^{111}\varepsilon_X$, ${}^{200}\varepsilon_X$, ${}^{220}\varepsilon_X$ and ${}^{311}\varepsilon_X$ with ϕ, the axial rotation angle along the X axis, under a deviatoric stress of $\sigma = (-0.5, 1, -0.5, 0, 0, 0)$ GPa expressed in the instrumental $(X'Y'Z')$ coordinate system for Au at 0 GPa.

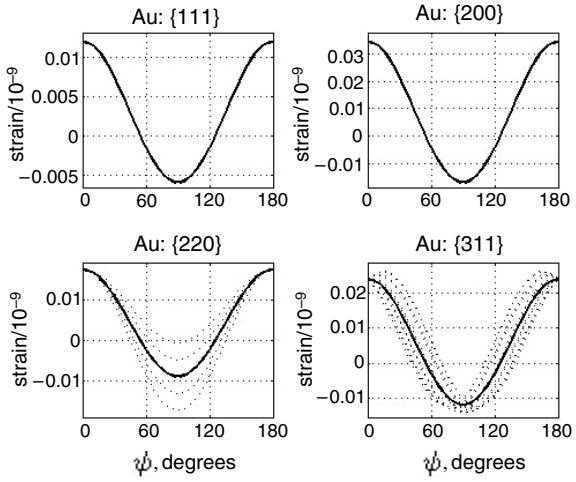

Figure 4. Lattice strain of hkl planes versus ψ. Dashed lines represent strain responses calculated numerically for various crystal grain orientations, ϕ. The solid line is the average of these, which is exactly consistent with the result obtained by equation (1).

equation (6) in which ${}^{hkl}S(\phi)_{XYZ}$ was replaced by ${}^{hkl}S(\psi)_{XYZ}$. Here we simply discuss the magnitude of the elastic strain in the hkl planes as a function of ψ apart from the diffraction condition. All the hkl planes have maximum compressional strain at $\psi = 0°$ where the hkl plane normal is parallel to the load axis, and minimum compressional strain at $\psi = 90°$ where the hkl plane normal is perpendicular to the load axis. In addition to this general feature, it is also clear that the calculated stress responses for {111} and {200} are independent of ϕ, while those for {110} and {311} are dependent on ϕ, which is consistent with the results by Funamori *et al* [28]. This figure also compares our results with those obtained from equation (1). The averaged lattice strain value over ϕ obtained from the numerical tensor calculation is exactly

the same as the results obtained from equation (1), proving that the analytical method using equation (1) gives the correct strain response of hkl planes when the polycrystalline material is free from preferred orientation.

4. Numerical procedures to simultaneously determine mean pressure and deviatoric stress

For the purpose of iterative calculations and to apply a generalized Hooke's law, we introduce a small variation in the mean pressure p, Δp, which is expressed as

$$\vec{\Delta p} = \begin{pmatrix} \Delta p \\ \Delta p \\ \Delta p \\ 0 \\ 0 \\ 0 \end{pmatrix}. \tag{7}$$

Δp does not depend on the selection of the axial coordinate. The mean pressure p is given as $p = p_0 + \Delta p$, where p_0 is a reference state of hydrostatic pressure. Now ε_X is defined with respect to p_0 (i.e., $\varepsilon_X = 0$ at $p = p_0$ and $\Delta\sigma = 0$), and thus ε_X can be expressed as a linear function of $\vec{\Delta p}$ and $\vec{\Delta\sigma}$ (generalized Hooke's law),

$${}^{hkl}\varepsilon_X = {}^{hkl}\varepsilon_1 = \sum_{m=1}^{6} {}^{hkl}S_{XYZ}(\phi)_{1m}(\vec{\Delta p}_m + \vec{\Delta\sigma}_m). \tag{8}$$

Because the deviatoric stress components depend on the selection of the axial coordinate, the deviatoric stress should be expressed by the x-ray diffraction (XYZ) coordinate system to calculate equation (8) (see the appendix for the derivation of equation (9)),

$$\vec{\Delta\sigma}_{XYZ} = \begin{pmatrix} -\frac{\cos^2\theta}{2} + \sin^2\theta \\ -\frac{\sin^2\theta}{2} + \cos^2\theta \\ -\frac{1}{2} \\ 0 \\ 0 \\ -\frac{3\cos\theta\sin\theta}{2} \end{pmatrix} \Delta\sigma = \vec{b}\,\Delta\sigma, \tag{9}$$

where the new column vector $\vec{b}$ is introduced to simplify the next equation. Now we can express equation (8) as

$$\begin{pmatrix} {}^{hkl}\varepsilon_X \\ * \\ * \\ * \\ * \\ * \end{pmatrix} = \begin{pmatrix} {}^{hkl}\varepsilon_1 \\ * \\ * \\ * \\ * \\ * \end{pmatrix} = {}^{hkl}\vec{\varepsilon} = {}^{hkl}S \cdot (\vec{\Delta p} + \vec{\Delta\sigma})$$

$$= \begin{pmatrix} S_{11} & S_{12} & S_{13} & S_{14} & S_{15} & S_{16} \\ S_{21} & S_{22} & S_{23} & S_{24} & S_{25} & S_{26} \\ S_{31} & S_{32} & S_{33} & S_{34} & S_{35} & S_{36} \\ S_{41} & S_{42} & S_{43} & S_{44} & S_{45} & S_{46} \\ S_{51} & S_{52} & S_{53} & S_{54} & S_{55} & S_{56} \\ S_{61} & S_{62} & S_{63} & S_{64} & S_{65} & S_{66} \end{pmatrix} \left[\begin{pmatrix} 1 \\ 1 \\ 1 \\ 0 \\ 0 \\ 0 \end{pmatrix} \Delta p + \begin{pmatrix} b_1 \\ b_2 \\ b_3 \\ b_4 \\ b_5 \\ b_6 \end{pmatrix} \Delta\sigma \right]$$

$$= \begin{pmatrix} (S_{11}+S_{12}+S_{13})\Delta p \\ * \\ * \\ * \\ * \\ * \end{pmatrix} + \begin{pmatrix} \sum_{m=1}^{6} S_{1m} b_m \Delta\sigma \\ * \\ * \\ * \\ * \\ * \end{pmatrix}$$
$$= \begin{pmatrix} {}^{hkl}A(\phi)\cdot\Delta p \\ * \\ * \\ * \\ * \\ * \end{pmatrix} + \begin{pmatrix} {}^{hkl}B\,(\phi)\cdot\Delta\sigma \\ * \\ * \\ * \\ * \\ * \end{pmatrix}. \tag{10}$$

Note that the S_{ij} matrix components are dependent on the hkl plane and the rotation angle ϕ along the X axis. However, for a cubic crystal, ${}^{hkl}A(\phi)$ is independent of the hkl planes and ϕ, i.e., ${}^{hkl}A(\phi) = A = 1/(3K)$ (K is the bulk modulus). ${}^{hkl}B(\phi)$ is different for each hkl and is significantly dependent on crystal orientation ϕ. However, for {111} and {200}, ${}^{hkl}B(\phi)$ is independent of ϕ, i.e., ${}^{hkl}B(\phi) = {}^{hkl}B$, as is clear from figure 3.

For the experimental data, we can define the strain in each of the hkl planes as

$${}^{hkl}E_X = -\frac{{}^{hkl}d_m - {}^{hkl}d_p}{{}^{hkl}d_p} \tag{11}$$

where ${}^{hkl}d_m$ is the observed d-value in the hkl plane by x-ray diffraction, and ${}^{hkl}d_p$ is the calculated d-value of the hkl plane for a reference hydrostatic pressure of p_0. The uppercase E is used to distinguish the observed strain from the calculated one. Now the problem can be simply expressed to solve the following simultaneous equations:

$$\begin{aligned} {}^{111}E_X &= A\cdot\Delta p + {}^{111}B\cdot\Delta\sigma \\ {}^{200}E_X &= A\cdot\Delta p + {}^{200}B\cdot\Delta\sigma. \end{aligned} \tag{12}$$

As the elastic constants are functions of pressure, the coefficients of A and ${}^{hkl}B$ are calculated using elastic constants and pressure derivatives of Au single crystal. In our case, we calculated A from an equation of state of Au [31, 32], while B was calculated based on single crystal elasticity data [33]. Although we examined other Au elasticity data [34–36], the differences were found to be as small as a few MPa both in the resulting mean pressure and the deviatoric stress.

Below is the procedure for the numerical iteration:

(i) assume a certain reference hydrostatic pressure p_0,
(ii) calculate ${}^{hkl}E_X$ from equation (11) and A and ${}^{hkl}B$ from equation (10) at $p = p_0$,
(iii) solve Δp and $\Delta\sigma$ in (12),
(iv) reset p_0 to $p_0 + \Delta p$,
(v) repeat (ii) to (iv) and continue iterative calculation until $\Delta p \to 0$.

Thus we obtain the mean pressure $p = p_0$ and deviatoric stress $\sigma = 1.5\Delta\sigma$ (see equation (3)). We refer to this numerical method using (111) and (200) as the '111–200' method. It is possible to conduct a least squares calculations by adding equations in (12) using the other (hkl). We refer to such least squares calculations as the '111–200–hkl' method (e.g., 111–200–220 method). In this case, however, we need to assume a specific distribution of crystal grain orientation, such as an isotropic one, in the sample to calculate ${}^{hkl}B$.

Table 1. The d-values of the Au pressure marker in the experiment. The values are shown in Å. The values in parentheses are the corresponding pressure values determined by a single index in GPa.

Run	d_{111}	d_{200}	d_{220}	d_{311}	d_{222}
ku0202	2.3222	2.0104	1.4217	1.2125	1.1607
	(7.82)	(8.01)	(7.96)	(7.92)	(8.01)
ku0204	2.3164	2.0061	1.4182	1.2097	1.1580
	(9.41)	(9.39)	(9.53)	(9.42)	(9.52)
ku0206	2.3145	2.0045	1.4172	1.2085	1.1570
	(9.94)	(9.93)	(10.01)	(10.03)	(10.06)
ku0208	2.3141	2.0040	1.4167	1.2082	1.1565
	(10.06)	(10.08)	(10.23)	(10.22)	(10.36)
ku0209	2.3266	2.0150	1.4247	1.2150	1.1632
	(6.64)	(6.61)	(6.66)	(6.67)	(6.68)

5. Example of data analysis and discussion: case study for gold

Diffraction data of Au were acquired as part of hydrostatic compression experiments of an aluminous magnesian silicate perovskite ($MgSiO_3$ containing 1 mol% Al_2O_3) using a DAC up to ∼10 GPa. An Au foil was prepared by squeezing Au powder between two anvils. A chunk of sintered polycrystalline perovskite and the Au foil were placed separately in a gasket hole filled with a 4:1 mixture of methanol and ethanol pressure medium [37]. *In situ* x-ray diffraction experiments were performed using synchrotron radiation x-rays at beam line 13-B2 of the Photon Factory, Tsukuba, Japan. An angle-dispersive diffraction technique was employed using an IP detector. The x-ray beam was monochromatized to the wavelength of 0.4429 ± 0.0002 Å using a Si(111) monochrometer. Details of the experimental procedure can be found in Kubo *et al* [38].

Table 1 shows the observed d-values for hkl planes of Au and the pressure values determined from individual d_{hkl} using the equation of state of Au [31, 32]. It is clear that the d-values of the 222 line are 0.006–0.045% smaller than expected from those of the 111 line, and as a result, pressures calculated from d_{111} and d_{222} differ by 0.04–0.30 GPa. The reason for this inconsistency is not clear. For this reason, we are aware of the limitation of the present analysis to yield unambiguous results using this experimental data set. However, a precision of the experimental d-values of the order of 0.0001 Å is required to obtain results with a precision of ∼0.1 GPa, as discussed later. Therefore, to test the performance of the present numerical analysis, we assume that either 111 or 222 exhibits the true d-value, and that the precision for the d-values is guaranteed in the figure of 0.0001 Å, even though the accuracy of the d-values might be of the order of 0.001 Å due to experimental uncertainties such as x-ray wavelength.

Table 2 shows an example of the calculated results for A, ${}^{hkl}B$, and d-values (run ku0208). The large difference between ${}^{222}B$ and ${}^{200}B$ enables us to conduct the present analysis. In the results from the 222–200 analysis, the expected d_p and d_m^{cal} for the 220 and 311 are shown. The d_m^{cal} for the 220 and 311 are in good agreement with d_m^{obs}, implying that the Au sample has a nearly isotropic grain orientation. Therefore, we also conducted the 222–200–311 and 222–200–220–311 analyses under the assumption of isotropic grain orientation. The results for 222–200–220–311 analysis are also shown in table 2 for comparison, showing excellent agreement between these results.

Table 3 shows the analytical results for the mean pressure and deviatoric stress. In the analyses including 222, both mean pressure and deviatoric stress show systematic evolution as a function of pressure, and deviatoric stresses are always compressional along the Y'

Table 2. Example of the calculated results of A, ^{hkl}B, and the d-values for ku0208 in the 222–200 and the 222–200–220–311 analyses.

222–200 analysis	A (Å GPa^{-1})	^{hkl}B	d_p (Å)	$d_m^{\rm cal}$	$d_m^{\rm obs}$
222	−1.4738e−3	4.2321e−3	1.1563	1.1565	1.1565
200	−1.4738e−3	12.993e−3	2.0028	2.0040	2.0040
220	−1.4738e−3	6.1491e−3	1.4162	1.4166	1.4167
311	−1.4738e−3	8.2579e−3	1.2077	1.2082	1.2082
222–200–220–311 analysis					
222	−1.4740e−3	4.2327e−3	1.1563	1.1565	1.1565
200	−1.4740e−3	12.994e−3	2.0028	2.0040	2.0040
220	−1.4740e−3	6.1498e−3	1.4162	1.4166	1.4167
311	−1.4740e−3	8.2588e−3	1.2077	1.2082	1.2082

Table 3. Comparison of pressure values determined by several methods. All data are shown in GPa. $P_{\rm ave}$ is the average of the pressures determined from each d_{hkl} without taking into account the effect of the deviatoric stress. The bulk moduli of aluminous perovskite, $K_{\rm PV}$, in the bottom row are based on the pressure values shown in each column.

Run	$P_{\rm ave}$	$P_{111-200}$ $\sigma_{111-200}$	$P_{222-200}$ $\sigma_{222-200}$	$P_{222-200-311}$ $\sigma_{222-200-311}$	$P_{222-200-220-311}$ $\sigma_{222-200-220-311}$
ku0202	7.94	7.72	8.00	7.97(10)	7.96(6)
		−0.05	−0.00	−0.003(16)	−0.005(11)
ku0204	9.45	9.41	9.59	9.57(5)	9.60(5)
		0.00	0.03	0.033(8)	0.038(8)
ku0206	10.00	9.94	10.13	10.14(4)	10.13(4)
		0.00	0.04	0.036(6)	0.033(6)
ku0208	10.19	10.05	10.49	10.49(2)	10.45(5)
		−0.01	0.07	0.071(3)	0.065(9)
ku0209	6.65	6.66	6.71	6.72(3)	6.72(2)
		0.01	0.02	0.019(5)	0.018(3)
$K_{\rm PV}$	233	230	237	237	236

direction within uncertainties, implying unexpected solidification of the methanol–ethanol mixture. On the other hand, the deviatoric stresses obtained from the 111–200 analysis are less than ±0.01 GPa except run ku0202, in which deviatoric stress is −0.05 GPa, indicating less compression in the Y' direction, which is not likely to develop in the compression process using a DAC. For this reason, we assume that the observed d-value of (222) is more consistent with those of the other hkl planes, and we discuss the possibility of solidification of the methanol–ethanol mixture during compression.

Figure 5 shows the evolution of the deviatoric stress as a function of the mean pressure based on the 222–200–311 analysis. The arrows indicate the time sequence of the experiment. We can see that deviatoric stress increases with mean pressure during the compression process, then decreases with mean pressure during the decompression process. It is known that a methanol–ethanol solution mixed in the eutectic volume ratio of 4:1 remains hydrostatic up to 10 GPa at room temperature. However, if the mixing ratio was not in the eutectic proportion, the solidification pressure could be less than 10 GPa according to the schematic phase diagram shown (figure 6). The appearance of deviatoric stress between 8.0 and 9.6 GPa can be

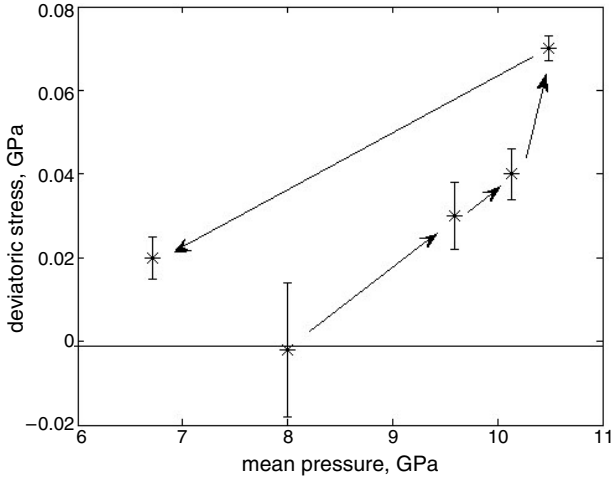

Figure 5. Mean pressure versus deviatoric stress of Au determined from the 222–200–311 analysis. The arrows show the time sequence of the data points.

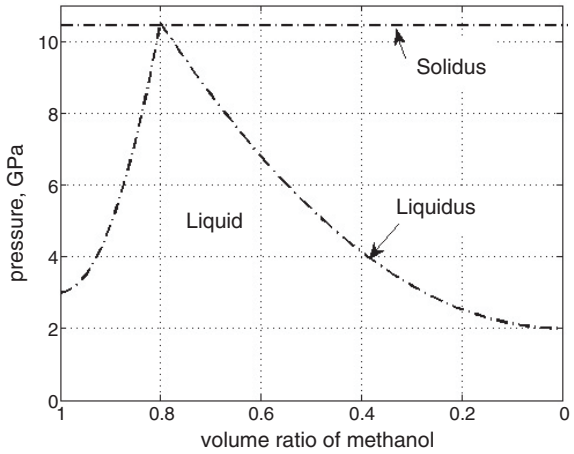

Figure 6. Schematic phase diagram for a methanol–ethanol system inferred from the freezing pressure of methanol and ethanol by Bridgman [48], and that of a 4:1 solution by Piermarini *et al* [37].

interpreted as partial solidification of the methanol–ethanol mixture, and the abrupt increase of the deviatoric stress between 10.1 and 10.5 GPa can be interpreted as the total solidification of the pressure medium, which is consistent with the freezing pressure of the eutectic composition of the mixture (4:1 methanol–ethanol in volume) [37]. On the other hand, a deviatoric stress of 0.02 GPa observed at the mean pressure of 6.7 GPa in the decompression process may be due to hysteresis of the solid–liquid transition in the methanol–ethanol mixture, and/or difference of the lowest bridging pressures of the sample in partially molten alcohol between the two diamond anvils due to the difference of thickness of the gasket in the loading and unloading processes.

The magnitude of the deviatoric stress supported by Au is ∼0.07 GPa at the highest mean pressure of 10.5 GPa (figure 5). If yielding occurs, the deviatoric stress should be limited to

the yield strength. The trend in the observed deviatoric stress shown in figure 5 is steeper than a linear function, suggesting that the yield strength of Au seems to be higher than 0.07 GPa at room temperature at ∼10 GPa. This is consistent with previous studies reporting a deviatoric stress of ∼0.2 GPa for Au at a corresponding pressure range [7, 8].

The original purpose of the diffraction experiment was to investigate the compressibility of aluminous silicate perovskite. As shown in table 3, revised pressure values by the 222-based analyses yield a larger bulk modulus from the equation of state fit for the aluminous perovskite, which is more consistent with the results obtained by Yagi *et al* [39] for the same material using He as a pressure medium (242 GPa). As discussed above, we can develop a consistent interpretation for the observed deviatoric stress in Au if we introduce solidification of the methanol–ethanol mixture during compression.

If we believe the 111-based results are more relevant than the 222-based analysis, one might adopt a completely different interpretation that Au was always compressed hydrostatically (except run ku0202, for some unknown reason). The largest difference of 0.001 Å between d_{111} and $2d_{222}$ in ku0208 (table 1) causes a difference of 0.08 GPa in deviatoric stress and 0.44 GPa in mean pressure (table 3). Therefore, if the precision of the experimental d-values is limited to the figure of 0.001 Å, we can rule out neither of these scenarios nor discuss the effect of deviatoric stress on P_{ave} in table 3. We therefore conclude that a precision of the order of 0.0001 Å is required to use the numerical tensor analysis in the case of the present Au study.

6. Concluding remarks

We demonstrate the feasibility of simultaneous determination of mean pressure and deviatoric stress from a numerical tensor analysis based on a generalized Hooke's law, if the precision of the experimental d-values is of the order of 0.0001 Å. This is the first demonstration of the simultaneous determination of mean pressure and deviatoric stress in high-pressure x-ray experiments by a numerical method without placing any assumptions (cf Meng *et al* [3]).

The present analysis suggests that even a small deviatoric stress (∼0.07 GPa) could yield a mean pressure error of ∼0.3 GPa using an Au pressure marker. The Au pressure scale could be very sensitive to stress, as discussed by Meng *et al* [3] in terms of large K/μ values (μ is the rigidity). If so, the stress sensitivity of the Au pressure marker would allow us to develop an internal stress sensor in a high-pressure apparatus.

Since Irifune *et al* [40] reported a relatively low pressure for the post-spinel transition in Mg_2SiO_4, there has been intensive debate on the reliability of the Au pressure scale [41–44]. The present work suggests that even small stresses (∼0.2 GPa) in the Kawai-type high-pressure apparatus [45] could yield ∼1 GPa errors in a pressure determination when an Au pressure marker is used, and this effect might in part explain the unusually low pressure for the post-spinel phase transition in Mg_2SiO_4 reported by Irifune *et al* [40].

Acknowledgments

The authors thank T S Duffy for thorough proofreading and comments, T Katsura, E Ito, and F Jiang for discussion and comments. Critical reviews by W A Bassett, H R Wenk and the anonymous reviewers have greatly improved the manuscript. AK conducted the experiments with the help of T Yagi, S Ono, and M Akaogi. This work was partially supported by a Grant-in Aid for Scientific Research No. 15204042 from the Japan Society for Promotion of Science and by a grant of the COE-21 program.

Appendix. Coordinate transformation of tensors

Although there are many textbooks on tensor analysis [46, 47], for the reader's convenience we present here some examples of tensor transformations. As long as the relative relationship between the two axis coordinates is explicit, we can transform the elastic compliance tensor expression from one coordinate system to another by applying the conversion rule for tensors. We specify the old coordinate system as $x_1x_2x_3$ and the new one as $x'_1x'_2x'_3$. The directional coefficients are defined by the inner product between the unit vectors as

$$a_{ij} = (\vec{e}'_i, \vec{e}_j), \qquad i, j = 1, 2, 3. \tag{A.1}$$

Any second-rank and fourth-rank tensor expressed in the old coordinate system can be converted to an expression in the new coordinate system such as

$$\begin{aligned} \sigma'_{ij} &= a_{ik}a_{jl}\sigma_{kl} \\ C'_{ijkl} &= a_{io}a_{jp}a_{kq}a_{lr}C_{opqr}. \end{aligned} \tag{A.2}$$

Note that the primes specify the expression in the new coordinate system. In spite of the simple conversion rule, the use of computers and computer programs such as MATLAB is inevitable for calculations.

Although the original tensor form is suitable for the conversion calculation, the 6×6 component notation is more convenient for representing tensors. For instance, the elastic stiffness matrix of an Au single crystal at ambient conditions is expressed as

$$C = \begin{pmatrix} 192.9 & 163.8 & 163.8 & 0 & 0 & 0 \\ 163.8 & 192.9 & 163.8 & 0 & 0 & 0 \\ 163.8 & 163.8 & 192.9 & 0 & 0 & 0 \\ 0 & 0 & 0 & 41.5 & 0 & 0 \\ 0 & 0 & 0 & 0 & 41.5 & 0 \\ 0 & 0 & 0 & 0 & 0 & 41.5 \end{pmatrix} \tag{A.3}$$

in GPa. Note that the above matrix is expressed in the xyz crystal coordinate system, which consists of the three four-fold symmetric axes of a cubic crystal. As to the conversion rule between the original tensor form and the 6×6 matrix, please check the literature for basic crystal elasticity.

The elastic compliance matrix, S, is used in the present stress analysis. It is easily obtained as the inversion matrix for the stiffness matrix C:

$$S = \begin{pmatrix} 23.55 & -10.81 & -10.81 & 0 & 0 & 0 \\ -10.81 & 23.55 & -10.81 & 0 & 0 & 0 \\ -10.81 & -10.81 & 23.55 & 0 & 0 & 0 \\ 0 & 0 & 0 & 24.10 & 0 & 0 \\ 0 & 0 & 0 & 0 & 24.10 & 0 \\ 0 & 0 & 0 & 0 & 0 & 24.10 \end{pmatrix} \tag{A.4}$$

in TPa^{-1}. Then we have to express the compliance matrix in the x-ray diffraction (XYZ) coordinate system. Let us consider the simplest case for the (200) plane. In this case, the xyz crystal coordinates are identical to the XYZ coordinates, and thus the expression of S in XYZ coordinates is given as (A.4). Then let us consider a 30° anticlockwise crystal grain rotation along the X axis, for example as shown in figure 2(b). The unit vectors for the XYZ coordinates are expressed as

$$e_X = (1,\ 0,\ 0), \qquad e_Y = (0,\ \cos(30°), -\sin(30°)), \qquad e_Z = (0, \sin(30°), \cos(30°)) \tag{A.5}$$

in the xyz coordinates associated with the crystal grain. The directional coefficients are given as

$$a_{ij} = \begin{pmatrix} 1 & 0 & 0 \\ 0 & \cos(30^\circ) & -\sin(30^\circ) \\ 0 & \sin(30^\circ) & \cos(30^\circ) \end{pmatrix} = \begin{pmatrix} 1 & 0 & 0 \\ 0 & 0.866 & -0.5 \\ 0 & 0.5 & 0.866 \end{pmatrix} \tag{A.6}$$

in matrix form. Note that the old expression for the compliance matrix S in xyz coordinates is the one shown as (A.4). After converting it to the corresponding fourth-rank tensor, we can apply the directional coefficients to obtain the new fourth-rank compliance tensor as shown in (A.2). The resulting compliance matrix expressed in XYZ coordinates is given as

$${}^{200}S_{XYZ}(30^\circ) = \begin{pmatrix} 23.55 & -10.81 & -10.81 & 0 & 0 & 0 \\ -10.81 & 15.18 & -2.45 & 9.66 & 0 & 0 \\ -10.81 & -2.45 & 15.18 & -9.66 & 0 & 0 \\ 0 & 9.66 & -9.66 & 57.57 & 0 & 0 \\ 0 & 0 & 0 & 0 & 24.10 & 0 \\ 0 & 0 & 0 & 0 & 0 & 24.10 \end{pmatrix}. \tag{A.7}$$

For the (111) plane, we can set the unit vectors of the XYZ coordinates to be

$$\begin{aligned} e_X &= \left(\frac{1}{\sqrt{3}}, \frac{1}{\sqrt{3}}, \frac{1}{\sqrt{3}}\right), \qquad e_Y = \left(-\frac{1}{\sqrt{2}}, \frac{1}{\sqrt{2}}, 0\right), \\ e_Z &= \left(-\frac{1}{\sqrt{6}}, -\frac{1}{\sqrt{6}}, \frac{\sqrt{2}}{\sqrt{3}}\right) \end{aligned} \tag{A.8}$$

in xyz coordinates (figure 2(c)). Note that the above case is an example in which the normal vector of the (111) plane coincides with the X axis. The resulting compliance matrix is given as

$${}^{111}S_{XYZ}(0^\circ) = \begin{pmatrix} 8.67 & -3.38 & -3.38 & 0 & 0 & 0 \\ -3.38 & 12.39 & -7.10 & 0 & -10.52 & 0 \\ -3.38 & -7.10 & 12.39 & 0 & 10.52 & 0 \\ 0 & 0 & 0 & 38.97 & 0 & -21.04 \\ 0 & -10.52 & 10.52 & 0 & 53.85 & 0 \\ 0 & 0 & 0 & -21.04 & 0 & 53.85 \end{pmatrix}. \tag{A.9}$$

Although the expressions are quite different from each other, (A.4), (A.7) and (A.9) are commonly expressed elastic behaviours of an Au single crystal.

Next, we calculate $\vec{\Delta\sigma}_{XYZ}$ (equation (9)). For this purpose, we temporarily express the deviatoric stress in the instrumental ($X'Y'Z'$) coordinate system as

$$\vec{\sigma}_{X'Y'Z'} = \begin{pmatrix} \sigma_1 \\ \sigma_2 \\ \sigma_3 \\ 0 \\ 0 \\ 0 \end{pmatrix}. \tag{A.10}$$

In the present diffraction geometry, the unit vectors of the XYZ coordinates with respect to $X'Y'Z'$ coordinates are expressed as

$$e_X = (\cos\theta, -\sin\theta, 0), \qquad e_Y = (\sin\theta, \cos\theta, 0), \qquad e_Z = (0, 0, 1). \tag{A.11}$$

Thus the directional coefficients (see (A.1)) are expressed in matrix form as

$$a_{ij} = \begin{pmatrix} \cos\theta & -\sin\theta & 0 \\ \sin\theta & \cos\theta & 0 \\ 0 & 0 & 1 \end{pmatrix}. \tag{A.12}$$

By applying the second-rank tensor transformation equation (A.2), we obtain the new expression for the deviatoric stress in XYZ coordinates:

$$\vec{\sigma}_{XYZ} = \begin{pmatrix} \sigma_1 \cos^2\theta + \sigma_2 \sin^2\theta \\ \sigma_1 \sin^2\theta + \sigma_2 \cos^2\theta \\ \sigma_3 \\ 0 \\ 0 \\ (\sigma_1 - \sigma_2)\cos\theta \sin\theta. \end{pmatrix} \tag{A.13}$$

By substituting σ_1, σ_2, and σ_3 in equation (A.13) with those in equation (3), we obtain an expression for the deviatoric stress in XYZ coordinates $\Delta\vec{\sigma}_{XYZ}$ (equation (9)).

References

[1] Singh A K and Kennedy G C 1974 *J. Appl. Phys.* **45** 4686
[2] Singh A K 1993 *J. Appl. Phys.* **73** 4278
[3] Meng Y, Weidner D J and Fei Y W 1993 *Geophy. Res. Lett.* **20** 1147
[4] Funamori N, Yagi T and Uchida T 1994 *J. Appl. Phys.* **75** 4327
[5] Kinsland G L and Bassett W A 1977 *J. Appl. Phys.* **48** 978
[6] Hemley R J, Mao H K, Shen G, Badro J, Gillet P, Hanfland M and Häusermann D 1997 *Science* **276** 1242
[7] Duffy T S, Shen G, Shu J, Mao H K, Hemley R J and Singh A K 1999 *J. Appl. Phys.* **86** 6729
[8] Duffy T S, Shen G, Heinz D L, Shu J, Ma Y, Mao H K, Hemley R J and Singh A K 1999 *Phys. Rev.* B **60** 15063
[9] Kavner A and Duffy T S 2001 *Geophys. Res. Lett.* **28** 2691
[10] Singh A K and Kenichi T 2001 *J. Appl. Phys.* **90** 3269
[11] Merkel S, Jephcoat A P, Shu J, Mao H-K, Gillet P and Hemley R J 2002 *Phys. Chem. Miner.* **29** 1
[12] Merkel S, Wenk H R, Shu J, Shen G, Gillet P, Mao H-K and Hemley R J 2002 *J. Geophys. Res.* **107** 2271
[13] Shieh S R, Duffy T S and Li B 2002 *Phys. Rev. Lett.* **89** 255507
[14] Kavner A and Duffy T S 2003 *Phys. Rev.* B **68** 144101
[15] Kavner A 2003 *Earth Planet. Sci. Lett.* **214** 645
[16] Akahama Y, Kawamura H and Singh A K 2004 *J. Appl. Phys.* **95** 4767
[17] Shieh S R, Duffy T S and Shen G 2004 *Phys. Earth Planet. Inter.* **143/144** 93
[18] Singh A K 2004 *J. Phys. Chem. Solids* **65** 1589
[19] Kiefer B, Shieh S R, Duffy T S and Sekine T 2005 *Phys. Rev.* B **72** 014102
[20] He D and Duffy T S 2006 *Phys. Rev.* B **73** 134106
[21] Speziale S, Shieh S R and Duffy T S 2006 *J. Geophys. Res.* **111** B02203
[22] Duffy T S, Hemley R J and Mao H K 1995 *Phys. Rev. Lett.* **74** 1371
[23] Shim S H, Duffy T S and Shen G Y 2000 *Phys. Earth Planet. Inter.* **120** 327
[24] Shim S H, Duffy T S and Shen G Y 2000 *J. Geophys. Res.* **105** 25955
[25] Liermann H P, Singh A K, Manoun B, Saxena S K and Zha C S 2005 *Int. J. Refract. Metals Hard Mater.* **23** 109
[26] Noyan I C and Cohen J B 1987 *Residual Stress* (Berlin: Springer)
[27] Hauk V 1997 *Structural and Residual Stress Analysis by Nondestructive Methods* (Amsterdam: Elsevier)
[28] Funamori N, Funamori M, Jeanloz R and Hamaya N 1997 *J. Appl. Phys.* **82** 142
[29] Gauthier M 2002 *High Pressure Res.* **22** 779
[30] Weidner D J, Vaughan M T, Ko J, Wang Y, Liu X, Yeganeh-Haeri A, Pacalo R E and Zhao Y 1992 *High-Pressure Research: Application to Earth and Planetary Sciences* ed Y Syono and M H Manghnani (Tokyo: Terra Scientific) p 13
[31] Heinz D L and Jeanloz R 1983 *J. Appl. Phys.* **55** 885
[32] Anderson O L, Isaak D G and Yamamoto S 1989 *J. Appl. Phys.* **65** 1534
[33] Hiki Y and Granato A V 1966 *Phys. Rev.* **144** 411
[34] Daniels W B and Smith C S 1958 *Phys. Rev.* **111** 713
[35] Golding B, Moss S C and Averbach B L 1967 *Phys. Rev.* **158** 637
[36] Biswas B N, Van't Klooster P and Trappeniers N J 1981 *Physica* B **103** 235
[37] Piermarini G J, Block S and Barnett J D 1973 *J. Appl. Phys.* **44** 5377
[38] Kubo A, Yagi T, Ono S and Akaogi M 2000 *Proc. Japan Acad.* B **76** 103
[39] Yagi T, Okabe K, Nishiyama N, Kubo A and Kikegawa T 2004 *Phys. Earth Planet. Inter.* **143/144** 81
[40] Irifune T, Nishiyama N, Kuroda K, Inoue T, Isshiki M, Utsumi W, Funakoshi K, Urakawa S, Uchida T, Katsura T and Ohtaka O 1998 *Science* **279** 1698

[41] Matsui M and Nishiyama N 2002 *Geophys. Res. Lett.* **29** 10
[42] Shim S H, Duffy T S and Kenichi T 2002 *Earth Planet. Sci. Lett.* **203** 729
[43] Tsuchiya T 2003 *J. Geophys. Res.* **108** 2462
[44] Fei Y, Li J, Hirose K, Minarik W, Van Orman J, Sanloup C, Van Westrenen W, Komabayashi T and Funakoshi K 2004 *Phys. Earth Planet. Inter.* **143/144** 515
[45] Kawai N and Endo S 1970 *Rev. Sci. Instrum.* **41** 1178
[46] Nye J F 1985 *Physical Properties of Crystals* (Oxford: Clarendon)
[47] Sands D E 1995 *Vectors and Tensors in Crystallography* (New York: Dover)
[48] Bridgman P W 1942 *Proc. Am. Acad. Arts Sci.* **74** 399